Photophysical Investigation into the Self-Organization in Pyrene-Based Urethane Methacrylate Comb Polymer

V. D. Deepak[‡] and S. K. Asha*[,†]

Polymer Science & Engineering Division, National Chemical Laboratory, Pune 411008, Maharashtra, India, Polymer Research Group, Chemical Sciences & Technology Division, National Institute for Interdisciplinary Science and Technology, Thiruvananthapuram 695019, Kerala, India

Received: February 16, 2009; Revised Manuscript Received: June 9, 2009

A side chain urethane methacrylate polymer with pendant pyrene units was synthesized and investigated for its self-organizing process in solution by UV−vis and fluorescence spectra and in film by scanning electron microscopy (SEM), transmission electron microscopy (TEM), and fluorescence microscopy. The polymer exhibited excimer emission centered at 476 nm, even at very dilute concentrations (10^{-6} M) as a consequence of the polymer design with pendant pyrene units on every side chain. A change in aggregation pattern was observed upon increasing the concentration to 10^{-4} M. New red-shifted peaks appeared in the UV−vis absorption spectra and the I_E/I_M ratio, and the peak I/peak III ratio showed a break around 10^{-4} M, suggesting formation of stable ground state aggregates. This was further confirmed by the SEM, TEM, AFM and fluorescence microscope studies, which showed the formation of vesicles in THF and giant spherical aggregates in THF/H_2O. The change in pattern of aggregate formation with concentration also coincided with a sudden increase in the intensity of the hydrogen bonded urethane N−H peak with concentration as recorded by solution FT-IR studies in THF.

Introduction

Molecular self-assembly, which is a thermodynamically controlled association of molecules into structurally ordered, stable aggregates making use of classical noncovalent interactions, has now been well-recognized as a means of developing nano- and microstructures.[1] Hydrogen bonding interactions, $\pi-\pi$ stacking interactions, dipole−dipole interactions, etc. have been traditionally made use of as tools for introducing the noncovalent interactions.[2,3] One major breakthrough that has been achieved in recent times for producing "large-area" ordered structures is the "breath-figure" approach which is the solvent-induced self-organization of polymer chains resulting in honeycomb structures as well as three-dimensional porous films.[4−7] The projected applications for these types of porous materials range from one extreme of applications in areas such as catalysis, sensors, in separation and adsorbent media to the other extreme of areas such as optical filters, photonic band gap materials, templates for the synthesis of nano-objects, carriers for drug delivery, etc.[8−10] Reports are available on the porous blue-light-emitting thin films of functionalized amphiphilic poly(*p*-phenylene)s which find potential applications in polymer optoelectronics and sensors.[11] Although initially it was assumed to be the prerogative of specially designed polymers such as star and rod−coil block copolymers incorporating styrene as one integral part of the polymer design, now there is plenty of evidence that other homopolymers such as poly(methylmethacrylate) and poly(carbonate) also could give rise to these uniformly patterned films.[12,13] The mechanistic aspects of this relatively simple patterning technique that has been discussed in the literature in general do not take into account the contribution, if any, of polymer structure factors that could aid in this patterning process. An exception to this was by Jenekhe et al., who interpreted the observation of microporous pattern in poly(phenylquinoline)-*block*-polystyrene rod−coil diblock copolymer system as due to self-organization of micellar aggregates into large-scale periodic microstructures.[7] The report on star-shaped, styrene-based vinyldiphenylquinoline polymers from the group of Stenzel also cites self-assembly of macromolecular materials as the origin of films with regular pore sizes.[14]

A direct correlation of self-organization in solution and morphology of solvent-cast films of the polymer sample could be obtained by introducing fluorescent probes into the polymer design. In fact, using confocal fluorescence microscopy, Stenzel et al. showed that poly(vinyldiphenylquinoline) star polymer formed fluorescent patterning with the most intense fluorescence coming from the rims, which was attributed to the preferential orientation of polymer chains with the fluorescent parts closer to the surface.[14] Fluorophores have been well-recognized as probes to study the conformational changes and molecular motions in polymers, since they open up a broad range of pathways through which one can trace the system behavior at the molecular level in addition to their typical photophysical as well as photochemical properties. Pyrene is one of the most widely used fluorophores for this purpose and displays a strong excimer emission at around 480 nm, a wavelength that is more than 50 nm longer than that of monomer emission.[15−17] The excimer formation in pyrene follows the classic Birk's scheme in which an excited pyrene can either emit a photon with its own lifetime or encounter a ground-state pyrene via diffusion and form a complex called an excimer. By monitoring the process of excimer formation between two pyrene groups, information about the nature of polymer association can be retrieved. However, the mode of incorporation of the probe also has an influence upon the type of information retrieved.[18] The information available in literature is mostly based on systems

* Corresponding author. Fax: 0091-20-25902615. E-mail: sk.asha@ncl.res.in.
‡ National Institute for Interdisciplinary Science and Technology.
† National Chemical Laboratory.

10.1021/jp901398e CCC: $40.75
Published on Web 08/13/2009

where the fluorescent units are attached at both ends of a monodisperse polymer. In contrast, Duhamel et al. have contributed a lot by describing the dynamics of encounters between pyrene pendants randomly attached onto various types of polymer backbones.[18−23] Randomly attached pendants can give much more valuable information by probing the entire polymer chain instead of just the two extreme ends.

Earlier, we had reported morphological studies of completely aliphatic side chain urethane methacrylate polymers.[24,25] The results of those preliminary studies encouraged us to investigate further into the self-organization behavior of the system by introducing a fluorescent probe as a handle. In the present work, we report photophysical as well as morphological studies on a urethane methacrylate polymer having pyrene as the pendant unit. Our present study on urethane methacrylate incorporated with pendant pyrene fluorophores is a step in this direction to understand, on one hand, the uniqueness of our polymer design that can form honeycomb patterns and vesicles in different solvents using pyrene as a fluorescent probe. On the other hand, it is also our intention to understand the type of information that can be retrieved by having pyrene pendant units precisely located on every single polymer chain, with the additional driving force of supramolecular organization in the form of hydrogen bonding forcing the units into close association. Unlike the commonly studied pyrene-based polymers in which pyrene is incorporated somewhere at the ends of the polymer chains or randomly distributed along the side chain, our polymer design presents the extreme situation of a probe molecule on every polymer chain, which is an interesting study by itself.

Experimental Section

Materials. Isophorone diisocyanate (IPDI), 2-hydroxyethyl methacrylate (HEMA), dibutyltindilaurate (DBTDL), 1-pyrene methanol, and benzoyl peroxide were purchased from Aldrich and used as such. *N*,*N*-dimethylformamide (DMF) was purified by keeping it overnight over KOH, followed by decanting and vacuum-distilling.[26]

Measurements. ^{1}H and ^{13}C NMR spectra of monomer and polymers were recorded using a 300-MHz Bruker NMR spectrophotometer in $CDCl_3$ containing small amounts of tetramethylsilane (TMS) as internal standard. The purity of the compounds was determined by JEOL JSM600 fast atom bombardment (FAB) high-resolution mass spectrometry. The purity of the monomers and the molecular weights of the polymers were determined by size exclusion chromatography (SEC) in tetrahydrofuran (THF) using polystyrene standards for the calibration. The GPC was calibrated with different polystyrene standards having molecular weights ranging from 2950 to 177 000 g/mol (Polymer Standards Service-USA, Inc.). A Waters 515 pump connected through three series of Styragel HR columns (HR-3, HR-4E, and HR-5E) and a Waters model 2487 dual wavelength UV−vis detector and a Waters 2414 differential refractometer were used for analyzing the samples. The flow rate of the THF was maintained at 1 mL throughout the experiments, and the sample solutions at very dilute concentrations were filtered and injected for recording the GPC chromatograms at 30 °C. Infrared spectra were recorded using a Perkin-Elmer Spectrum One FT-IR spectrophotometer. The liquid samples or dilute solution of the solid samples in dichloromethane were spread over KBr plates, and their spectra were recorded.

UV−vis spectra were recorded using a Perkin-Elmer Lambda 35 UV−vis spectrometer. The emission studies were performed by a SPEX Fluorolog F112X spectrofluorometer using 1 nm slit width. The fluorescence quantum yields of the polymer were determined in THF using quinine sulfate in 0.1 M H_2SO_4 (ϕ = 0.546) as the standard. The optical density at λ_{max} was maintained at 0.1 ± 0.05 to avoid reabsorption artifacts. The thermal stability of the polymers was determined using a DTG-60 Shimadzu thermogravimetric analyzer at a heating rate of 10 °C/min in nitrogen. Differential scanning calorimetry (DSC) measurements were performed on a DSC Perkin Elmer Pyris 6 DSC instrument at a heating rate of 10 °C/min under a nitrogen atmosphere. Typically, 2−3 mg of samples was placed in an aluminum pan, sealed properly, and scanned from −30 to 250 °C. The instrument was calibrated with indium standards before measurements.

Scanning Electron Microscopy (SEM). Polymer samples for the measurements were provided with a thin gold coating using a JEOL JFC-1200 fine coater. The probing side was inserted into a JEOL JSM-5600 LV scanning electron microscope for taking photographs. The sample preparation method adopted was as follows: A solvent/nonsolvent mixture of THF/H_2O was first mixed in a 9:1 ratio, and then 10 mg of polymer was dissolved in 1 mL of this mixture, resulting in a stable and clear polymer solution. Twenty microliters of this solution was placed on a glass slide, and the solution was allowed to evaporate at room temperature in air. All films were prepared at atmospheric pressure without air flow.

Transmission Electron Microscopy (TEM). Transmission electron microscopy was performed on an FEI, TEC NAI 30 G2 S-TWIN microscope with an accelerating voltage of 100 kV. For TEM measurements, a drop of the polymer solution (10^{-4} molar solution of THF/H_2O = 9:1 mixture) was deposited directly onto a Formvar-coated copper grid. No staining treatment was performed for the measurement.

Atomic Force Microscopy (AFM). AFM images were taken by a multimode scanning probe microscope equipped with Nanoscope IV controller from Veeco Instrument Inc., Santa Barbara, in the contact mode using a SiN probe, with maximum scan size 10 μm × 10 μm and with vertical range of 2.5 μm. For the AFM studies, 1 × 10^{-4} M filtered solution in THF or THF/H_2O = 9:1 mixture was drop-cast on silicon wafers.

Fluorescent Microscopy. Fluorescence microscopy was done on a Nikon Eclipse E-600 using excitation filter EX-330-380, emission filter BA-400, and dichromatic mirror DM-400.

Synthesis of 2-Methyl Acrylic Acid 2-[1,3,3-Trimethyl-5-(pyren-2-ylmethoxycarbonylamino)-cyclohexylmethylcarbamoyloxy]-ethyl Ester (Isophoronediisocyanate-HEMA-Pyrene: IHP). IPDI (1.71 g, 7.69 × 10^{-3} mol) in 8 mL of dry DMF was taken in a 50 mL, two-necked, round-bottomed flask, and the contents were cooled with ice. HEMA (1 g, 7.69 × 10^{-3} mol) was added dropwise with constant stirring under nitrogen. The reaction was allowed to proceed under ice cold conditions for 0.5 h, followed by room temperature stirring for 2 h. Three drops of dibutyltin dilaurate (DBTDL) was added as catalyst, followed by dropwise addition of pyrene methanol in 7 mL DMF (1.78 g, 7.69 × 10^{-3} mol) under ice cold conditions. It was left stirring in ice for an additional 0.5 h and then was heated to 60 °C for 6 h. The contents were poured into 200 mL of water and were extracted with dichloromethane. The extract was washed with water, dried over anhydrous sodium sulfate, concentrated, and dried in a vacuum oven at 60 °C for 12 h. Yield: 4.1 g (91%). ^{1}H NMR (300 MHz, $CDCl_3$) δ ppm: 8.37−8.00 (m, 9H, Ar-**H**), 6.04, 5.49 (2s, 2H, CH_2=C), 5.81 (s, 2H, −OCH_2 next to pyrene ring), 5.63−4.39 (m, N**H**), 4.32 (s, 4H, O−CH_2−CH_2−O of HEMA), 3.21 (b, 1H, C**H**−NH−COO of IPDI), 2.87 (b, 2H, −CH_2−NH−COO of

SCHEME 1: Synthesis of Homopolymer PIHP

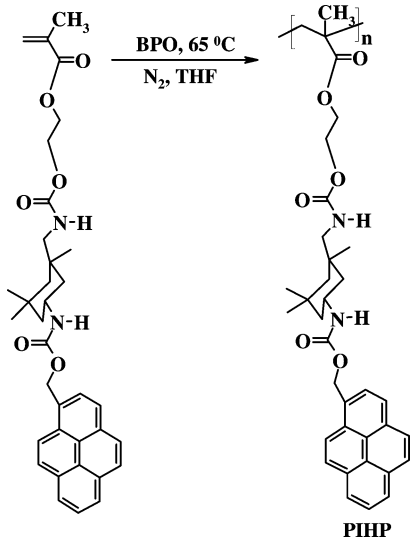

PIHP

IPDI), 1.96 (s, 3H, C**H**$_3$− of HEMA), 1.73−0.79 (aliphatic protons of IPDI). ^{13}C NMR (75 MHz, $CDCl_3$) δ ppm: 166.82, 156.75, 155.09, 135.51, 134.02, 130.69, 130.21, 128.95, 127.47, 126.64, 125.28, 124.12, 122.56, 64.58, 62.55, 62.13, 61.92, 54.42, 53.47, 46.41, 45.51, 44.13, 41.58, 41.03, 35.84, 34.46, 31.15, 29.29, 29.08, 27.16, 22.72, 22.62, 22.29, 17.86. FT-IR (cm^{-1}): 3388, 2953, 2862, 1715, 1637, 1531, 1455, 1388, 1366, 1297, 1243, 1171, 1059, 1030, 899, 815, 713. (MW: 584). FAB HRMS M + 1: 585.05.

Free Radical Polymerization of IHP. IHP (1.0 g, 1.71×10^{-3} mol) and benzoylperoxide (0.012 g, 5.13×10^{-5} mol) were taken in THF (5 mL) in a 10 mL round-bottomed flask provided with a water condenser. The reaction mixture was purged with nitrogen for 10 min. The polymerization was carried out by stirring the contents at 65 °C for 12 h. The viscous liquid was cooled and precipitated into methanol. Yield: 0.75 g (75%). THF SEC: $M_n = 30\,900$. PDI = 2.5. ^{1}H NMR (300 MHz, $CDCl_3$) δ ppm: 8.29−7.92 (m, 9H, Ar-**H**), 5.72 (s, 2H, −OC**H**$_2$ next to pyrene ring) 4.81−4.29 (b, N**H**), 3.72 (b, 4H, O−C**H**$_2$−C**H**$_2$−O of HEMA), 2.92−0.85 (m, other aliphatic protons).^{13}C NMR (75 MHz, $CDCl_3$) δ ppm: 176.92, 156.83, 155.66, 131.58, 131.09, 130.59, 129.39, 128.03, 127.63, 127.27, 125.95, 125.32, 124.55, 123.01, 67.89, 64.89, 54.81, 46.88, 46.15, 44.67, 41.65, 36.33, 34.97, 31.71, 29.58, 27.54, 25.54, 23.21. FT-IR (KBr, cm^{-1}): 3382, 3043, 2951, 1715, 1528, 1462, 1388, 1360, 1303, 1240, 1139, 1057, 897, 847, 800, 772, 712, 680, 625.

Results and Discussion

Synthesis and Characterization. The monomer IHP (IPDI−HEMA−Pyrene) was synthesized by a similar procedure described elsewhere.[24] It was polymerized using 3 mol % benzoyl peroxide as initiator in tetrahydrofuran (THF) as solvent at 65 °C, as shown in Scheme 1. The monomer and polymer were characterized using different spectroscopic techniques, such as ^{1}H and ^{13}C NMR, FT-IR, and FAB-mass (Supporting Information Figure S1). The ^{1}H NMR spectrum of the monomer (IHP) and its polymer (PIHP) with the peaks labeled are given in Figure 1. In the NMR spectrum of the monomer, the sharp, well-separated peaks at 6.14 and 5.60 ppm correspond to the methacrylic double bond protons. The N−**H** proton peaks at ∼5 ppm are complicated due to the fact that isophoronediisocyanate (IPDI) is a mixture of cis and trans isomers (72% cis and 28% trans). The peaks labeled "f" corresponding to the −OC**H**$_2$ next to the pyrene unit matched perfectly in intensity with the double bond methacrylic peaks in IHP, signifying that the different halves of the molecule had coupled stochiometrically, as expected. Upon polymerization, the double bond methacrylic peaks disappeared, and the pyrenyl protons shifted by ∼0.1 ppm, probably due to the enhanced electronic interaction between the pyrenyl groups in the polymer. The ^{13}C NMR spectra of monomer and polymer are given in the Supporting Information (Figure S2). The peaks at 134.02 ppm and 125.28 ppm correspond to the olefinic carbon atoms, which are completely absent in the polymer spectrum. The polymerization could be followed by the FT-IR spectra also by following the disappearance of the methacrylic double bond peaks at 1630 and 815 cm^{-1} (Supporting Information, Figure S3). The molecular weight was determined by gel permeation chromatography using polystyrene standards and THF as eluent (Supporting Information, Figure S4). The polymer was purified by repeated reprecipitation from THF into methanol. The polymer showed monomodal distribution with number average molecular weight (M_n) of 30 900 with a polydispersity of 2.5. The thermal properties were analyzed by using thermogravimetric analysis (TGA) and DSC. TGA analysis showed that the polymer was stable up to 285 °C. The 10% weight loss temperature was 283 °C. DSC analysis showed that the polymer was amorphous with a T_g of 143 °C (Supporting Information, Figures S5 and S6).

Photophysical Studies. The photophysical studies of the polymer were done using absorption and fluorescence spectroscopic techniques in THF as the solvent. Figure 2 shows the UV−vis absorption spectra of a 0.1 OD (∼10^{-6} M) solution of monomer (IHP) and polymer (PIHP) recorded in THF. The absorption spectra show the characteristic vibronically resolved spectra of pyrene with three vibronic bands at 312, 326, and 343 nm corresponding to $^1L_a \leftarrow {}^1A$ electronic transitions.[17,27] Figure 2 also shows the fluorescence spectra recorded for IHP and PIHP in THF, by exciting at 343 nm, corresponding to the (0, 0) transition and normalized at 375 nm. The emission spectra show peaks characteristic of the emission of excited pyrene monomer at 375 and 395 nm. In addition to the above-mentioned peaks, they also show an additional structureless emission band at 476 nm that is characteristic of pyrene excimer emission. This broad emission between 450 and 550 nm is usually assigned to inter- or intramolecular excimer emission.[28] This emission is usually observed when the concentration of pyrene is high enough ($10^{-4}-10^{-3}$ M) to form excited state species. Comparing the monomer IHP and polymer PIHP, the polymer had very intense excimer emission at ∼ 470 nm, in contrast to the weak excimer emission for IHP for the same concentration of pyrene (10^{-6} M). This is a consequence of the polymer design having pyrene units at each hanging segment that are driven closer by the hydrogen bonding as well as by the $\pi-\pi$ aromatic interactions. Therefore, intrachain excimer formation is expected to occur even at very dilute conditions.

Table 1 gives the fluorescence quantum yields measured in THF at room temperature using quinine sulfate as the standard ($\phi_r = 0.546$ in 0.1 M H_2SO_4). The quantum yield was calculated using the equation[29]

$$\phi_s = \phi_r[F_sA_r/F_rA_s](n_r/n_s)^2$$

where ϕ_s is the fluorescence quantum yield of the sample, F is the area of the emission peak, n is the refractive index of solution, and A is the absorbance of the solution at the exciting wavelength. The subscripts r and s denote reference and sample,

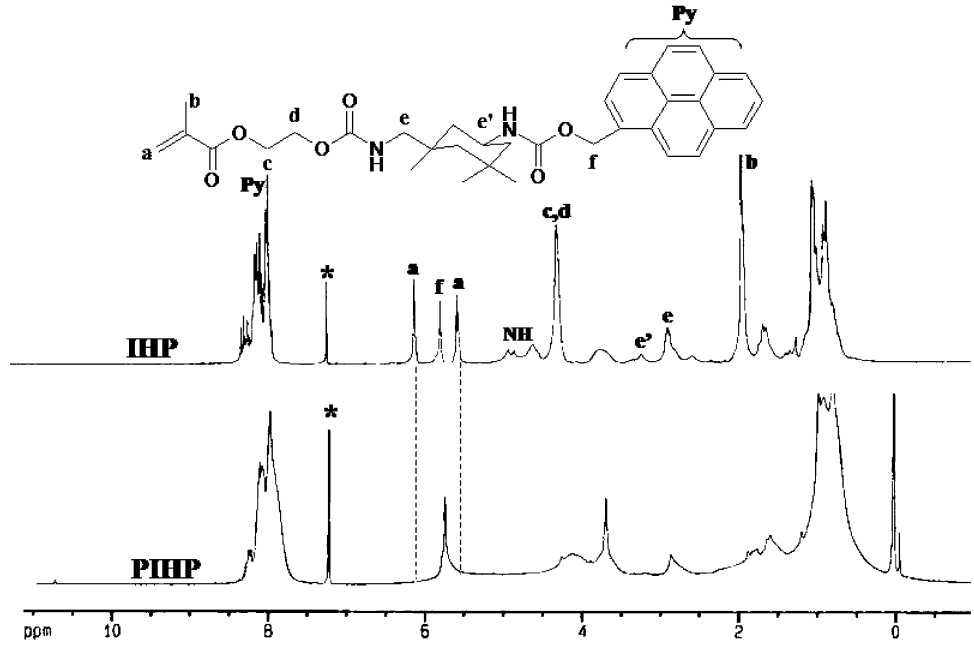

Figure 1. ^{1}H NMR spectra of monomer IHP and corresponding homopolymer PIHP.

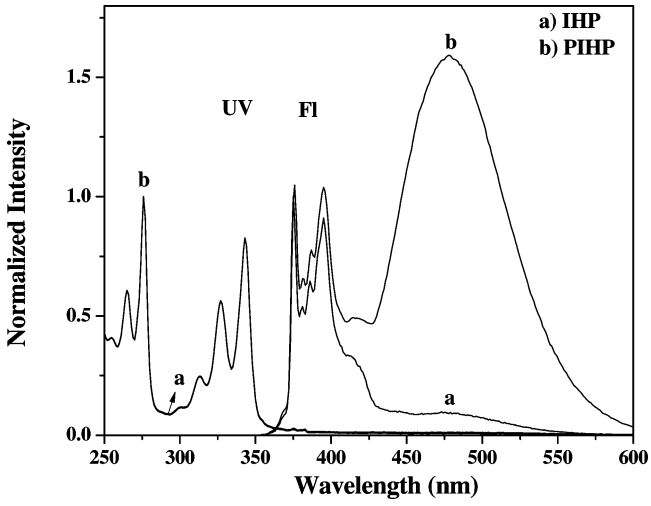

Figure 2. Combined UV−vis and fluorescence spectra of (a) IHP and (b) PIHP recorded in tetrahydrofuran (0.1 OD solutions).

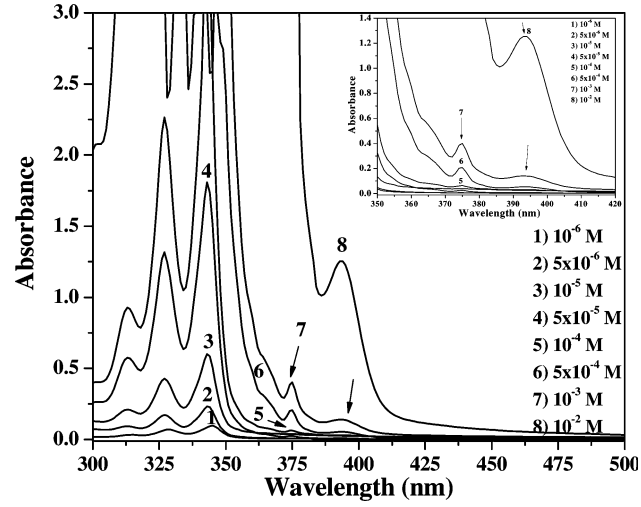

Figure 3. UV−visible absorption spectra of the polymer PIHP in different concentrations in THF.

TABLE 1: Photophysical Properties of the IHP and PIHP in THF (~0.1 OD)

	in THF (nm)		
sample	λ_{max} (abs) (nm)	λ_{max} (em)[a] (nm)	ϕ_{FL}[b]
IHP	343	375, 382, 387, 395, 415, 476	0.19
PIHP	343	375, 382, 387, 395, 415, 476	0.48

[a] Excitation wavelength is 343 nm. [b] Calculated using 0.1 OD quinine sulfate solution as standard. Excitation wavelength is 343 nm.

respectively. The reported fluorescence quantum yield value for the starting material 1-pyrenemethanol (PyOH) is 0.1.[30] Under our experimental conditions, the fluorescence quantum yield value obtained for PyOH in THF was 0.17, and that of monomer IHP was 0.19. The polymer PIHP had a quantum yield value of $\phi_f = 0.48$. This nearly 3-fold increase in fluorescence quantum yield compared to the starting material pyrene methanol (PyOH) or IHP is due to the excimer formation.

To understand the nature of pyrene association in the polymer, absorption and emission studies were done at different concentrations ranging from 10^{-6} to 10^{-2} M in THF. Figure 3 shows the variable concentration absorption spectrum of PIHP in THF. It was found that as the concentration of the polymer solution increased, an additional red-shifted peak appeared and broadening in the absorption spectrum occurred, which are indications of pyrene preassociation.[17] When the concentration increased from 10^{-6} to 10^{-4} M, a new peak appeared at 375 nm (see the expanded spectra in the inset of Figure 3). On further increasing the concentration to 10^{-3} M, the intensity of the peak at 375 nm increased, and another new peak appeared at 395 nm because of strong aggregation.

The variable concentration fluorescence spectra of the polymer recorded in THF at the two excitation wavelengths of 343 (A) and 395 (B) nm is given in Figure 4. The emission spectra obtained upon excitation at 343 nm, (plot A, top) show the typical sharp monomer emission peaks at 375, 382, 387, 395, and 415 nm (λ_M) and a broad excimer emission peak at 476 nm (λ_E). The 395 nm excitation (plot B, bottom), on the other hand, exhibited a peak maximum at 446 nm, which is usually attributed to pyrene dimer emission or excimer species with

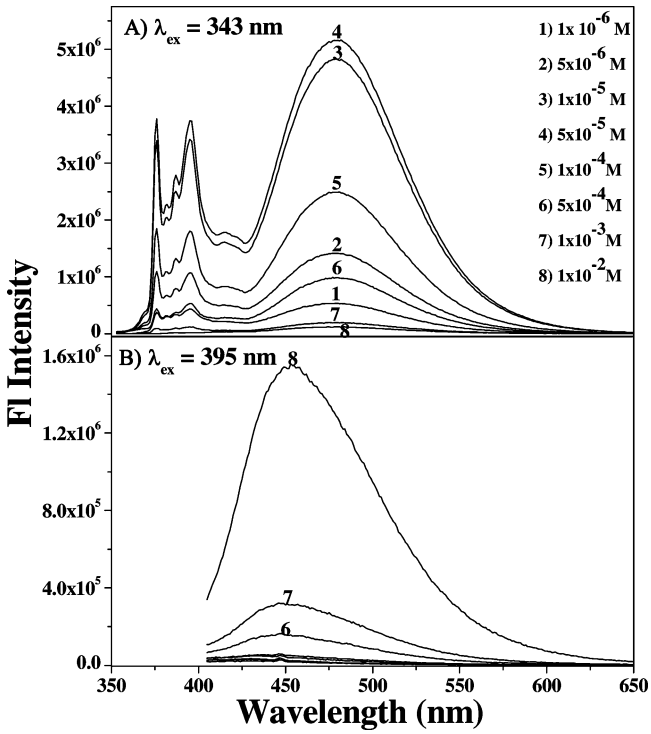

Figure 4. Variable concentration emission spectra of the polymers PIHP at excitation wavelengths of 343 (A) and 395 (B) nm in THF.

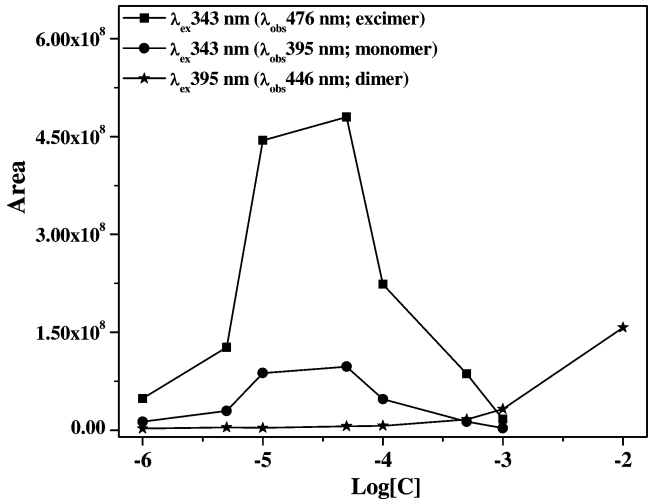

Figure 5. Plot of area of fluorescence intensity at the monomer and excimer or dimer peak as a function of log [*C*] for PIHP in THF.

partial overlap of pyrene units.[31,32] Figure 5 shows the plot of the area of fluorescence intensity for the monomer (395 nm), excimer (476 nm), and dimer (446 nm) as a function of concentration for the polymer. The areas of fluorescence intensity for monomer and excimer were obtained by deconvolution of the emission spectra at 343 nm excitation, and that for dimer was obtained from the emission spectra at 395 nm excitation. It can be seen that the excimer (476 nm) and monomer (395 nm) emission upon excitation at 343 nm increased initially and then decreased as the concentration increased beyond 10^{-4} M. The monomer (395 nm) emission intensity was much less as compared to the excimer emission. The dimer emission at 446 nm upon excitation at 395 nm started increasing only from 10^{-4} M onward and increased steadily and continued without quenching, even at 10^{-2} M. This could be directly visualized by the naked eye itself from the intense blue-green emission in the case of PIHP, in contrast to the blue emission of pyrene methanol (Supporting Information Figure S7).

The quenching of monomer and excimer emission at high concentration could be attributed to the "inner filter effect" because at such high concentrations, the optical density (OD) at the exciting wavelength (i.e., 343 nm) is so high (>3) that it results in a decrease in the intensity of the excitation at the point of observation.[33] Table 2 gives the OD at the different wavelengths used for excitation and observation of fluorescence intensity in this study. It can be seen that the fluorescence intensity increased linearly with OD until ~0.6 OD (10^{-5} M), reached a maximum ~1.8 OD (5×10^{-5} M), and decreased thereafter. However, in the case of the emission at 446 nm upon excitation at 395 nm, the OD is only 1.2, even at the highest concentration of 10^{-2} M. Therefore, at 395 nm, the dimer emission showed a continuous increase in intensity, even at such high concentrations. The most important information that can be obtained from the plot in Figure 5 is that beyond 10^{-4} M, pyrene dimers were also present in the solution. Normally, dimer emission at 446 nm is very difficult to observe since the exited dimer (D*) is very unstable, and its radiationless transfer to the excimer state (E*) occurs much faster than the radiative process of dimer emission.[31,34]

Excimer emissions are known to be concentration-dependent. The ratio of the intensities of excimer (476 nm) to monomer (395 nm) emission is used to measure the efficiency of excimer formation.[17] A large I_E/I_M ratio indicates that the pyrenes are located close to one another. The plot of I_E/I_M versus the concentration of the polymer solution obtained from the 343 nm excitation (Figure 4 A) is shown in Figure 6, and the values are given in Table 2. From the plot, it can be seen that there was not much change in the I_E/I_M ratio with concentration until 10^{-4} M; beyond 10^{-4} M, the value started increasing and attained the highest of 6.32 at 10^{-2} M. One can rule out selective reabsorption of fluorescence emission at 395 or 476 nm to be the origin of this break in the I_E/I_M ratio at high concentration because the OD at both wavelengths is much less than 1.0, even until 10^{-3} M (see Table 2). The OD at the exciting wavelength of 343 nm is, however, >3.0 at the higher concentrations of 10^{-4}, 5×10^{-4}, and 10^{-3} M, and therefore, a reduction in fluorescence emission intensity is expected at these concentrations due to the inner filter effect, as discussed earlier. However, this reduction in fluorescence emission is expected to affect both 395 and 476 nm emission equally and not preferentially or selectively for either of them. On the other hand, this observed break in the I_E/I_M ratio is similar to that reported for tied-up systems such as the pyrene end labeled poly(dimethylsiloxane) reported by Torkelson et al.[35] Under dilute conditions, the I_E/I_M ratio is independent of concentration, and excimer formation is determined by local pyrene concentration rather than overall pyrene concentration. The interaction between pyrene moieties is almost exclusively intrachain and dynamic in nature, resulting in the I_E/I_M ratio's being independent of concentration. The excimer emission until 10^{-4} M is driven by diffusive interaction of an excited state pyrene with a ground state pyrene. The dynamic nature of the excimer origin can be confirmed by measurement of excitation spectra collected at the monomer (395 nm) and excimer (476 nm) emission wavelengths. When the excimer formation is by the diffusive encounter between two pyrene units, the two excitation spectra must superimpose.[17,36,37] On the other hand, if the excimers are static in nature, that is, preassociated pyrene molecules, then the monomer and excimer excitation spectra will be red-shifted by 1−4 nm.[17] Figure 7

TABLE 2: Optical Densities at Various Wavelengths and I_E/I_M (E = 476 nm and M = 395 nm) Values and I_1/I_3 (I_1 = 375 nm and I_3 = 386 nm) Values of PIHP in THF at Different Concentrations

		OD					PIHP	
[C], M	log[C]	at 343 nm	at 375 nm	at 386 nm	at 395 nm	at 476 nm	I_E/I_M in THF	I_1/I_3 in THF
10^{-6}	−6	0.09	0.006	0.005	0.005	0.001	1.23	1.18
5×10^{-6}	−5.3	0.23	0.007	0.004	0.003	0.002	1.31	1.27
10^{-5}	−5	0.60	0.026	0.008	0.008	0.003	1.41	1.27
5×10^{-5}	−4.3	1.81	0.039	0.029	0.026	0.004	1.37	1.29
10^{-4}	−4	3.04	0.064	0.032	0.030	0.010	1.38	1.31
5×10^{-4}	−3.3	3.81	0.208	0.046	0.053	0.013	1.81	0.89
10^{-3}	−3	>3	0.401	0.121	0.137	0.018	1.67	0.97
10^{-2}	−2	>3	>3	1.012	1.227	0.045	6.32	

compares the normalized excitation spectra recorded while monitoring the excimer (476 nm (curve 1)) and monomer (395 nm (curve 2)) emission wavelength for PIHP at (A) 10^{-6} M concentration. At 10^{-6} M, the excitation spectrum monitored at both the monomer and the excimer wavelengths were identical as well as superimposable on one another. This indicated that the excimer formation was dynamic in nature at these low concentrations. The concentration dependence of the I_E/I_M ratio beyond 10^{-4} M suggested interchain ground state aggregate formation. In fact, new red-shifted peaks were observed in the variable concentration UV−vis absorption spectra recorded in THF beyond 10^{-4} M. The presence of ground state dimers or aggregates can be confirmed by excitation spectra measurements. Unfortunately, at concentrations above 10^{-4} M, the excitation spectrum became broadened and distorted due to the inner filter effect (see supplementary figure S8). However, a 3 nm red shift was observed for the excitation spectrum recorded at the excimer compared to that recorded at the monomer wavelength and additionally, the excitation spectra also showed a new peak at 375 nm (indicated by arrow) similar to the observation in the variable concentration UV−vis absorption spectra at 10^{-4} M. The excitation spectra thus gave proof of the fact that ground state aggregates were formed beyond a concentration of 10^{-4} M.

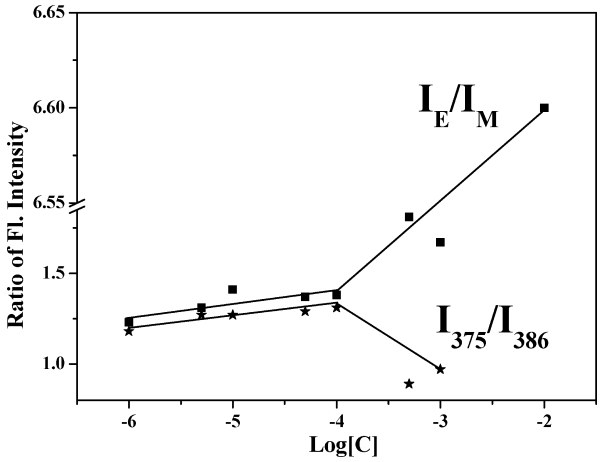

Figure 6. Excimer to monomer intensity ratio (I_E/I_M E = 476 nm and M = 395 nm) and peakI/peakIII (I_1/I_3; I_1 = 375 nm and I_3 = 386 nm) intensity ratio for 343 nm excitation spectra in THF as a function of increasing concentration. (The line is for guidance only).

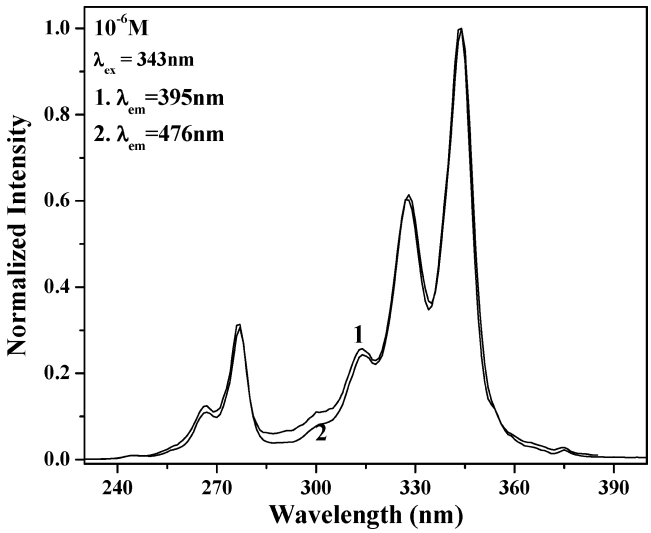

Figure 7. Normalized excitation spectra of PIHP recorded while monitoring the excimer (476 nm; **1**) and monomer (395 nm; **2**) emission at 10^{-6} M concentrations in THF.

Additional information regarding the pyrene local environment can be obtained from the ratio of the first and third vibronic bands of monomer emission. These fine structures are very sensitive to the solvent microenvironment, and generally the intensity ratio of peak I/peak III (375 nm/386 nm) serves as a measure of solvent polarity. This peak ratio can be qualitatively taken as a measure of the extent of interaction between the pyrene system and the solvent. The values of peak I/peak III at different concentrations in THF are given in Table 2 and plotted along with the I_E/I_M ratio in Figure 6. The value of this ratio at 10^{-2} M could not be obtained, since at this high concentration, the monomer emission was completely quenched. This value was ∼1.2 at 10^{-6} M, which decreased to ∼0.9 beyond 10^{-4} M. A value of 0.6 is reported in the literature for pyrene in a hydrophobic environment.[38,39] This sharp change in behavior at 10^{-4} M concentration also coincides with the observation of a new peak in the UV−vis absorption spectra and also the sudden change in the I_E/I_M ratio. This indicates that beyond 10^{-4} M concentration, higher-order aggregates were formed with pyrene shielded from the rest of the polymer.

The excited state behavior of the excimer forming homopolymers is quite complex considering the various conformational and configurational possibilities. Free radical polymerization usually gives rise to atactic polymers, which means that both isotactic and syndiotactic diad configurations will be present. Kamat et al. had shown that poly(1-vinyl pyrene) exhibited more than one type of excimer emission due to a different extent of overlap of neighboring pyrene units present in their atactic polymer.[40] The fluorescence lifetime measurements can give important information regarding the nature of the emitting species. This will be taken up and studied in the future for PIHP.

Hydrogen Bonding Studies Using FT-IR. Pyrene has characteristic strong peaks in the FT-IR spectrum at 841 and 710 cm^{-1} attributed to a C−H wagging vibration.[41] When pyrene is involved in strong $\pi-\pi$ interactions, a shift to higher wavenumbers[42] occurs in this peak. The FT-IR spectra of PIHP

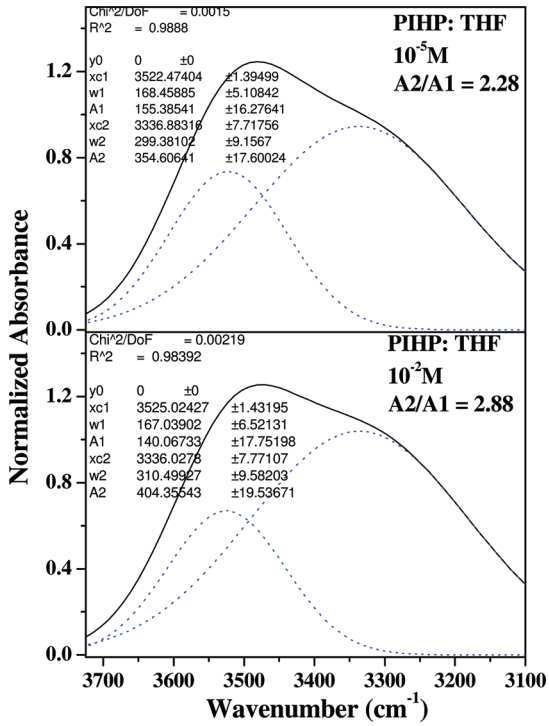

Figure 8. Expanded N−H region of the FT-IR spectra of PIHP at two different concentrations, 1×10^{-5} (top) and 1×10^{-2} (bottom), in THF. Dotted line shows the deconvoluted peaks corresponding to free and hydrogen bonded N−H. Inset shows the fit details obtained using Origin Pro 8.

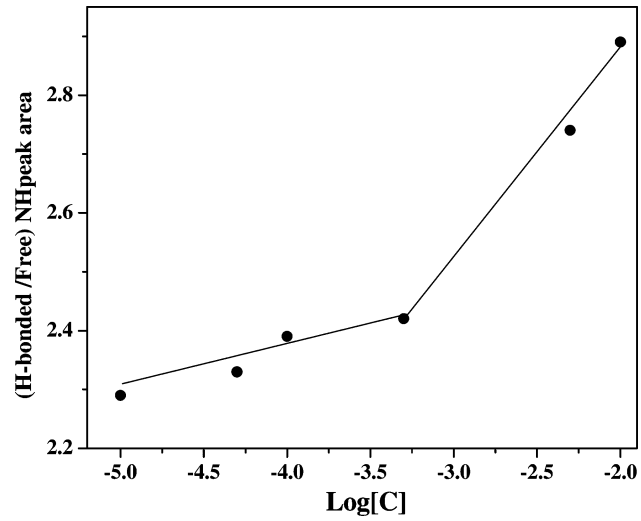

Figure 9. Plot of hydrogen bonded to free N−H peak area as a function of concentration (log[*C*]). The line is just a guidance to the eye.

were recorded as a solid powder on a KBr pellet and also drop-cast into a film from THF/H_2O 9:1 (v/v) solvent mixture and then recorded as solid powder on a KBr pellet. In both cases, prominent peaks were observed at 846 and 712 cm^{-1} respectively (Supporting Information, Figure S9) suggesting strong $\pi-\pi$ interactions.

An important aspect of the urethane methacrylate polymer design was its ability to form hydrogen bonding interactions. The urethane linkage in the polymer side chains is expected to induce hydrogen bonding, both intra- and interchain, in the system. This hydrogen bonding interaction is also expected to play a role in bringing the pyrene moieties into close proximity to each other and also in directing the morphology in solvent-cast polymer films. The extent of hydrogen bonding interactions was determined by carrying out variable concentration (1×10^{-5} to 1×10^{-2} M) FT-IR measurements in THF. Generally, the peak at higher wavenumber, ~3500 cm^{-1}, is assigned to the free stretching vibration of the N−H group in the urethane linkage, and the band at lower wavenumber, ~3300 cm^{-1}, is assigned to the hydrogen-bonded N−H stretching vibration.[43] The variable concentration FT-IR spectra were deconvoluted using OrginPro 8 to obtain the area of the peak under the free and N−H bonded peak. The deconvolution of the peak at two extremes, 1×10^{-5} M and 1×10^{-2} M, showing the contribution from the free and N−H bonded peaks is given in Figure 8. The ratio of the hydrogen bonded to free N−H peak areas was plotted as a function of concentration (log[*C*]) and is given in Figure 9. The connecting line is provided for guidance only. From the figure, it can be seen that the ratio varied very little (2.2−2.4) under dilute conditions, but increased linearly with concentration to a maximum value of 2.89 at 1×10^{-2} M. The linear increase in the hydrogen bonded to the free N−H peak area at high concentrations for PIHP is in accordance with the observation from the photophysical studies that suggested formation of static dimers and higher aggregates at high concentrations resulting from interchain interactions. The break in the hydrogen bonded to the free N−H peak ratio as a function of concentration occurred at ~5×10^{-4} M, which is very similar to the observation from the photophysical studies also.

Morphology. Earlier, we had reported the self-organization of nonfluorescent side chain urethane methacrylate polymers having bulky terminal units into vesicles and compound micelles from THF or THF/H_2O solvent mixture. The self-organization characteristics of the polymer PIHP were studied using different solvents, such as THF and THF/H_2O. The absorption and emission data in THF/H_2O solvent mixture are given in the Supporting Information, Figures S10−S11.

Thin films of the homopolymer of PIHP were prepared on glass slides by drop-casting the polymer solution (10 mg/mL; ~0.02 molar) in different solvents, such as THF and THF/H_2O (9:1) at room temperature. The polymer films were kept at room temperature for 12 h for the complete evaporation of the solvents. The factors that influence the film preparation, such as the sample concentration, humidity, temperature, mode of film preparation, etc., were maintained identical for all the studies.[44,45] Scanning electron microscopic (SEM) images of polymer PIHP in THF are shown in Figure 10. Observations under an optical microscope (data not shown) and a scanning electron microscope revealed the formation of hexagonally packed micropores formed in THF with a narrow size distribution. The films were opaque upon solvent casting onto glass substrates. PIHP formed regular hexagonal pores with average diameters of 1.2 ± 0.16 μm, and the pores were separated by thin walls having average thicknesses of 0.65 ± 0.073 μm (see Table 3). A change in the concentration of the polymer solution caused changes in the regularity of the films with dilute solutions, forming very irregular pores. Therefore, the SEM studies were carried out for a concentration of 10 mg/mL. Figure 11c and d shows the SEM pictures for films drop-cast from the THF/H_2O 9:1 solvent mixture. With this slight incorporation of water, the honeycomb morphology was totally transformed, yielding in its place solid spheres having an average size of 1.55 ± 0.31 μm. Water being a poor solvent for pyrene compared to THF, the polymer attained a spherical shape with pyrene shielded inside, thus registering a hydrophobic environment.

The polymer was subjected to TEM analysis. The polymer films for TEM measurements were prepared by drop-casting polymer solution onto a Formvar-coated copper grid without

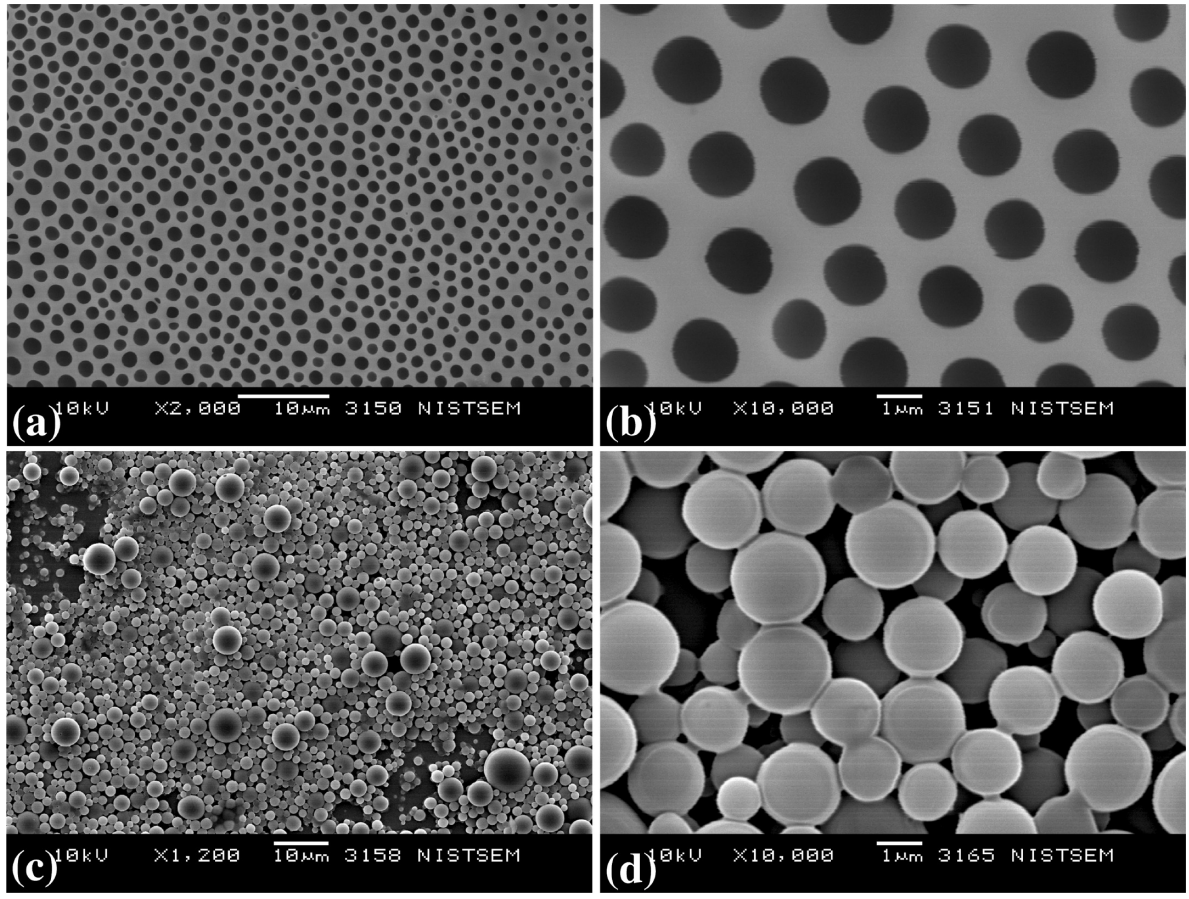

Figure 10. SEM images of PIHP 10 mg/mL THF (a and b), 10 mg/mL THF/H_2O = 9:1 v/v. (c and d) Prepared by drop-casting 20 μL solution onto a glass slide.

TABLE 3: Morphological Data of PIHP

polymer solution	SEM	TEM	AFM	Fl microscope
THF	1.2 ± 0.16 μm[a]	1.21 ± 0.158 μm[d]	750 nm[g]	
	0.65 ± 0.073 μm[b]	50 ± 12 nm[e]		
THF/H_2O	1.55 ± 0.31 μm[c]	207 ± 53 nm[f]	850 nm[h]	1.2 μm[i]

[a] The size of the pores calculated from SEM image. [b] The size of the wall thickness calculated from SEM image. [c] The size of the spheres calculated from SEM image. [d] The size of the vesicles calculated from TEM image. [e] The size of the wall thickness of vesicles calculated from TEM image. [f] The size of the spheres calculated from TEM image. [g] The average size of the vesicles calculated from AFM image. [h] The average size of the spheres calculated from AFM image. [i] The size of the spheres measured directly from the instrument.

any special staining. Homopolymer solutions (10^{-4} molar) in THF and THF/H_2O were used for the TEM measurements; the images are given in Figures 11 and 12. The TEM image of polymer films obtained from THF shows the formation of vesicles (Figure 11a and b). The Supporting Information, Figure S14, shows some more TEM images of vesicles prepared for different films of the same sample. The vesicular structures were identified because of the obvious contrast between the contour and the center of the aggregates, as illustrated in the literature.[46−48] The vesicles had an average size of 1.21 ± 0.158 μm, with a wall thickness of 50 ± 12 nm. The vesicular nature of the features was further confirmed by the AFM image shown in Figure 12c and d of 1×10^{-4} M PIHP in THF dropcast onto silicon wafers. In some cases, deformation is observed resulting in a crater-like morphology which is in agreement with their hollow vesicular structure.[49] Supporting Information, Figure S15 shows some more AFM images of vesicles. The size of the vesicle is in the range of 0.5−0.9 μm. Figure 12a and b shows the TEM images of PIHP in THF/H_2O. Similar to the observation in SEM, it showed the presence of rigid spheres with average size of 207 ± 53 nm. The images showed the fusion of smaller spheres into larger spheres and were very similar to those described by Eisenberg et. al as large compound micelles.[50−52] Figure 12 c and d shows the AFM images of 1×10^{-4} M PIHP in THF/H_2O drop-cast onto silicon wafers. It also confirmed the existence of spheres with an average size of 850 nm throughout the entire area (see Supporting Information Figure S16).

The difference in morphology for solutions from THF observed in SEM and TEM is surprising. Earlier also, we had reported similar observation of vesicles in TEM giving honeycomb patterns in SEM images. Chang et al. has reported for poly(vinyl phenol)-*block*-polystyrene that at higher concentrations of the polymer solutions, the vesicles transformed into ordered honeycomb morphology. They also reported vesicles in TEM (at low concentration) and three-dimensional honeycomb structure in SEM (at higher concentration).[53]

A comparison of the morphology exhibited by PIHP with that exhibited by similar nonfluorescent systems that we had reported earlier will help throw some light on the uniqueness of this polymer structure design that assists self-assembly. In the systems that we had reported earlier, in which cycloaliphatic units such as tricyclodecane (TCD) or adamantane were used in place of the fluorescent pyrene, SEM images showed honeycomb pattern formation, and TEM showed vesicles in THF/water 9:1 solvent combination for films prepared under

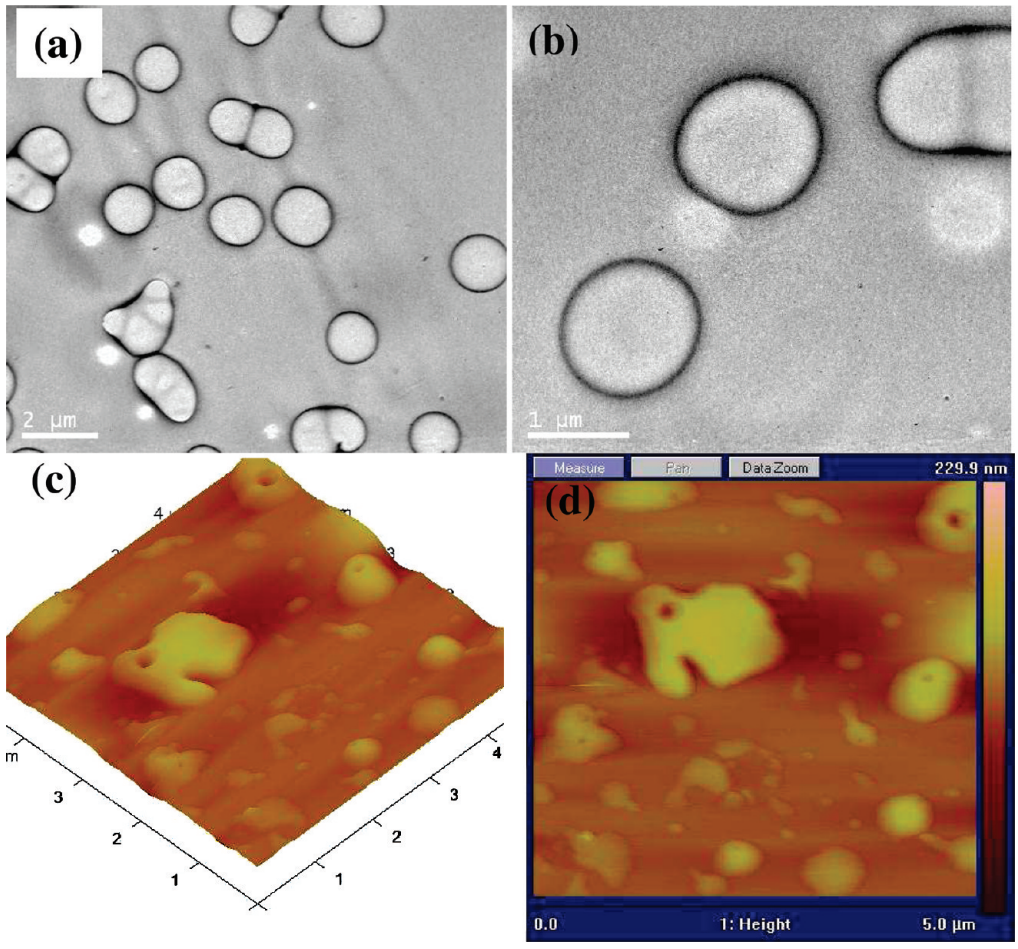

Figure 11. (a, b) TEM images of PIHP prepared by drop-casting onto a Formvar-coated copper grid and (c, d) AFM images prepared by drop-casting onto a silicon wafer. Concentration is 10^{-4} M solution in THF.

conditions identical to that reported here.[24] Upon fine-tuning the rigidity/solubility of the system by formation of diblock copolymer with styrene (TCD-*b*-styrene), SEM showed formation of spheres, and TEM images showed large compound micelles from THF/water 9:1 combination.[25] Unlike the above observation, in the case of the pyrene system (PIHP), the homopolymer itself formed vesicles in THF and large compound micelles in THF/water 9:1 solvent combination. The ability to self-organize is inherent in the polymer design in the form of hydrogen bonding interaction of the urethane linkage or the rigidity/solubility balance of the various units. The incorporation of pyrene into the polymer design results in fine-tuning this rigidity/solubility balance so that the homopolymer itself can now exhibit morphologies that were earlier attainable only in a block copolymer configuration.

Pyrene being a highly fluorescent probe, the polymer PIHP was subjected to fluorescent microscopy. For fluorescent microscopic measurements, 10 mg of polymer sample was dissolved in 1 mL of THF/H_2O in 9:1 ratio. Twenty microliters of the solution was drop-cast on a glass slide, and the dried film was observed under the fluorescence microscope that uses an excitation filter in the 330−380 nm regions. The fluorescent microscopic images in two different magnifications are given in Figure 13. Light bluish fluorescent spheres having average size 1.2 μm were observed under the fluorescence microscope, which is in agreement with SEM and TEM images.

To further prove the role of hydrogen bonding in the self-assembly process, the SEM of polymer PIHP was recorded in the THF/H_2O 9:1 mixture as well as in the THF/H_2O 9:1 mixture with four drops of trifluoroacetic acid (TFA). The samples were prepared by dissolving 10 mg of sample in 1 mL of THF/H_2O 9:1 as a control and 10 mg of sample in 1 mL of the THF/H_2O 9:1 mixture with 4 drops (40 μL) of trifluoroacetic acid also added to it. Twenty microliters of each of the solutions was drop-cast onto cover glass slides and allowed to evaporate under ambient conditions. The films were allowed to evaporate under ambient conditions without air flow. SEM images recorded in the absence (a) and presence (b) of added TFA are given in the Supporting Information, Figure S17. TFA is known to disrupt hydrogen bonding, and the films also had a glassy and transparent appearance upon addition of few drops of TFA. The FT-IR spectra also were recorded for these films drop-cast from THF/H_2O 9:1 and THF/H_2O with 40 μL of TFA added to it and are given in the Supporting Information, Figure S18, showing the expanded N−H region along with the deconvolution peaks. The ratio of the hydrogen bonded to free N−H peak area was 0.8 for the former, which reduced to 0.6 in the presence of TFA. Although the added TFA was not sufficient to disrupt the entire hydrogen bonding, it was enough to destroy the self-organization into spheres.

Conclusion

A side chain urethane methacrylate polymer having pendant pyrene units on each side chain was synthesized and characterized. The polymer exhibited the characteristic pyrene excimer emission at 476 nm in THF in the dilute condition arising from intrachain interactions, but at higher concentrations, interchain

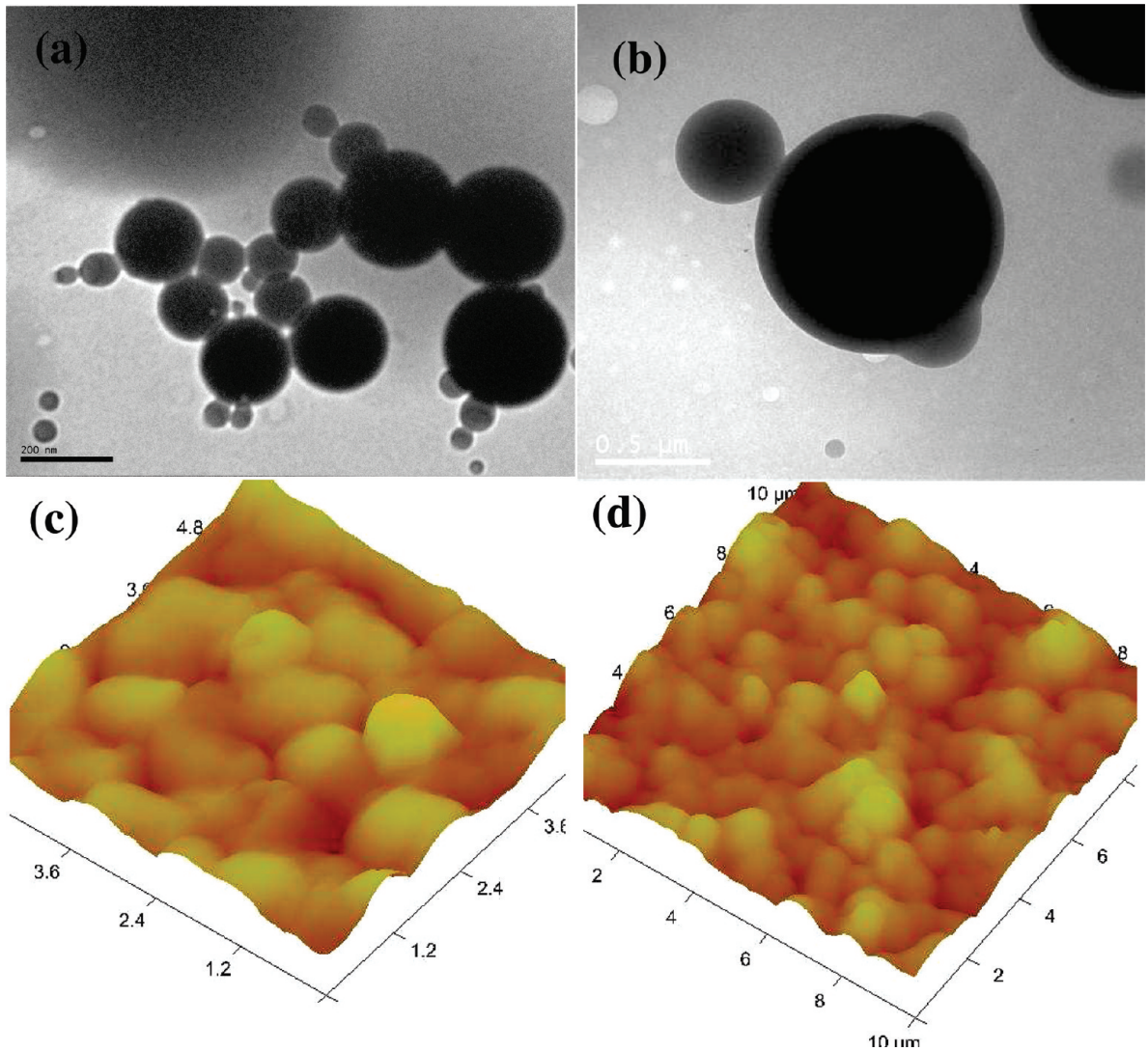

Figure 12. (a, b) TEM images of PIHP prepared by drop-casting onto a Formvar-coated copper grid and (c, d) AFM images prepared by drop-casting onto a silicon wafer. Concentration is 10^{-4} M solution in THF/H_2O = 9:1 v/v.

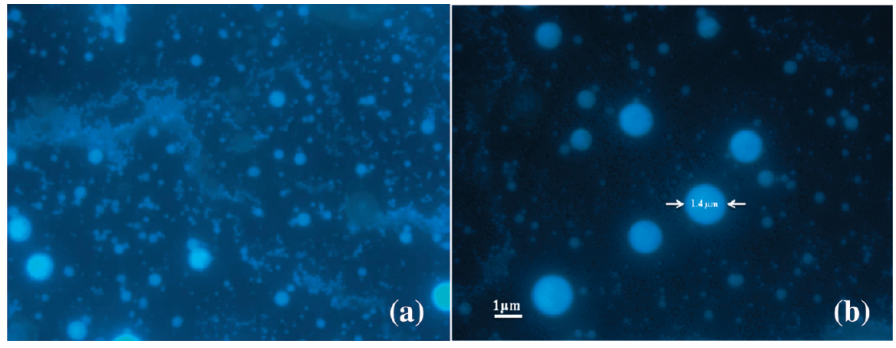

Figure 13. Fluorescence microscopy images of PIHP in THF/H_2O = 9:1 v/v prepared by drop-casting 20 μL of solution onto a glass slide. SEM images of polymer PIHP prepared by drop-casting 20 μL of solution onto a glass slide. (A) 10 mg/mL THF/H_2O = 9:1 v/v and (B) 10 mg/mL THF/H_2O = 9:1 v/v with four drops (~40 μL) of TFA.

interactions also occurred, resulting in stable ground state aggregate formation. Drop-cast films of the sample from THF as solvent showed vesicles, whereas those drop-cast from the THF/H_2O 9:1 solvent combination formed microspheres or compound micelles, as observed in the TEM images. This was also confirmed by fluorescence microscopy, which showed the presence of fluorescent microspheres. Such compact structures are primarily a consequence of extensive hydrophobic interactions between the bulky hydrophobes, but hydrogen bonding of the urethane units may also contribute to the formation of these structures to some extent.

Acknowledgment. We thank the network project NWP0023 and in-house project MLP 013526 for financial support. The authors thank Dr. Peter Koshy and Mr. M. R. Chandran, NIIST, for SEM and Dr. V. S. Prasad and Mr. Robert Philip NIIST for

TEM analysis. We also thank Dr. T. R. Santhoshkumar RGCB Trivandrum for fluorescence microscopic analysis and Mr. K. Vivekanand, Materials Chemistry Division, NCL-Pune for AFM measurements. D.V.D. thanks CSIR-New Delhi, India, for a Senior Research Fellowship.

Supporting Information Available: FAB-HRMS of monomer, ^{13}C NMR of monomer and polymer, GPC chromatogram of polymer, TGA and DSC plots, UV−vis and fluorescence studies in THF/H_2O, etc.This material is available free of charge via the Internet at http://pubs.acs.org.

References and Notes

(1) Whitesides, G. M.; Mathias, J. P.; Seto, C. T. *Science* **1991**, *254*, 1312.
(2) Deepa, P.; Jayakannan, M. *J. Polym. Sci., Part A: Polym. Chem.* **2007**, *45*, 2351.
(3) Jancy, B.; Asha, S. K. *Chem. Mater.* **2008**, *20*, 169.
(4) Widawski, G.; Rawiso, B.; Francois, B. *Nature* **1994**, *369*, 387.
(5) Chen, D.; Jiang, M. *Acc. Chem. Res.* **2005**, *38*, 494.
(6) Srinivasarao, M.; Collings, D.; Philips, A.; Patel, S. *Science* **2001**, *292*, 79.
(7) Jenekhe, S. A.; Chen, X. L. *Science* **1999**, *283*, 372.
(8) de Boer, B.; Stalmach, U.; van Hutten, P. F.; Melzer, C.; Krasnikov, V. V.; Hadziioannou, G. *Polymer* **2001**, *42*, 9097.
(9) Martin, C. R. *Science* **1994**, *266*, 1961.
(10) Imada, M.; Noda, S.; Chutinan, A.; Tokuda, T.; Murata, M.; Sasaki, G. *Appl. Phys. Lett.* **1999**, *75*, 316.
(11) Nurmawati, M. H.; Renu, R.; Ajikumar, P. K.; Sindhu, S.; Cheong, F. C.; Sow, C. H.; Valiyaveettil, S. *Adv. Funct. Mater.* **2006**, *16*, 2340.
(12) Wang, Y.; Liu, Z.; Huang, Y.; Han, B.; Yang, G. *Langmuir* **2006**, *22*, 1928.
(13) Zhao, B.; Zhang, J.; Wu, H.; Wang, X.; Li, C. *Thin Solid Films* **2007**, *515*, 3629.
(14) Kowollik, C. B.; Dalton, H.; Davis, T. P.; Stenzel, M. H. *Angew. Chem.* **2003**, *115*, 3792.
(15) Shazmann, B.; Alhashimy, N.; Diamond, D. *J. Am. Chem. Soc.* **2006**, *128*, 8607.
(16) Xiao, X.; Xu, W.; Zhang, D.; Xu, H.; Liu, L.; Zhu, D. *New J. Chem.* **2005**, *29*, 1291.
(17) Winnik, F. M. *Chem. Rev.* **1993**, *93*, 587.
(18) Ingratta, M.; Duhamel, J. *Macromolecules* **2007**, *40*, 6647.
(19) Duhamel, J.; Kanagalingam, S.; O'Brien, T. J.; Ingratta, M. W. *J. Am. Chem. Soc.* **2003**, *125*, 12810.
(20) Mathew, A. K.; Siu, H.; Duhamel, J. *Macromolecules* **1999**, *32*, 7100.
(21) Kanagalingam, S.; Ngan, C. F.; Duhamel, J. *Macromolecules* **2002**, *35*, 8560.
(22) Vangani, V.; Duhamel, J.; Nemeth, S.; Jao, T.-C. *Macromolecules* **1999**, *32*, 2845.
(23) Prazeres, T. J. V.; Beingessner, R.; Duhamel, J.; Olesen, K.; Shay, G.; Bassett, D. R. *Macromolecules* **2001**, *34*, 7876.
(24) Deepak, V. D.; Asha, S. K. *J. Phys. Chem. B* **2006**, *110*, 21450.
(25) Deepak, V. D.; Asha, S. K. *J. Polym. Sci., Part A: Polym. Chem.* **2008**, *46*, 1278.
(26) Tyman, J. H. P. *J. Chromatogr.* **1975**, *111*, 277.
(27) Prado, E. A.; Yamaki, S. B.; Atvars, T. D. Z.; Zimerman, O. E.; Weiss, R. G. *J. Phys. Chem. B* **2000**, *104*, 5905.
(28) Birks, J. B. *Photophysics of Aromatic Molecules*; Wiley: New York, 1970.
(29) Feng, L.; Chen, Z. *Polymer* **2005**, *46*, 3952.
(30) Guldi, D. M.; Menna, E.; Maggini, M.; Marcaccio, M.; Paolucci, D.; Paolucci, F.; Campidelli, F.; Prato, M.; Rahman, G. M. A.; Schergna, S. *Chem.—Eur. J.* **2006**, *12*, 3975.
(31) Sluch, M. I.; Vitukhnovsky, A. G.; Petty, M. C. *Thin Solid Films* **1996**, *284−285*, 622.
(32) Kimura, M.; Miki, N.; Suzuki, D.; Adachi, N.; Tatewaki, Y.; Shirai, H. *Langmuir* **2009**, *25*, 776.
(33) Lakowicz, J. R. *Principles of Fluorescence Spectroscopy*, 3rd ed.; Springer: New York, 2006.
(34) Frank, R. S.; Merkle, G.; Gauthier, M. *Macromolecules* **1997**, *30*, 5397.
(35) Kim, S. D.; Torkelson, J. M. *Macromolecules* **2002**, *35*, 5943.
(36) Kim, S. K.; Bok, J. H.; Bartsch, R. A.; Lee, J. Y.; Kim, J. S. *Org. Lett.* **2005**, *7*, 4839.
(37) Winnik, M. A.; Bystryak, S. M.; Liu, Z.; Siddiqui, J. *Macromolecules* **1998**, *31*, 6855.
(38) Kalyanasundaram, K.; Thomas, J. K. *J. Am. Chem. Soc.* **1977**, *99*, 2039.
(39) Dong, D. C.; Winnik, M. A. *Can. J. Chem.* **1984**, *62*, 2560–2565.
(40) Todesco, R. V.; Basheer, R. A.; Kamat, P. V. *Macromolecules* **1986**, *19*, 2390.
(41) Zhang, Y.; Yuan, S.; Zhou, W.; Xu, J.; Li, Y. *J. Nanosci. Nanotechnol.* **2007**, *7*, 2366.
(42) Tanhuanpa, K.; Cheng, K. H.; Anttonen, K.; Virtanen, J. A.; Somerharju, P. *Biophys. J.* **2001**, *81*, 1501.
(43) Asha, S. K.; Schenning, A. P. H. J.; Meijer, E. W. *Chem.—Eur. J.* **2002**, *8*, 3353.
(44) Stenzel, M. H. *Aust. J. Chem.* **2002**, *55*, 239.
(45) Bormashenko, E.; Pogreb, R.; Stanevsky, O.; Bormashenko, Y.; Stein, T.; Gendelman, O. *Langmuir* **2005**, *21*, 9604.
(46) Mu, M.; Ning, F.; Jiang, M.; Chen, D. *Langmuir* **2003**, *19*, 9994.
(47) Deepa, P.; Jayakannan, M. *J. Polym. Sci., Part A: Polym. Chem.* **2008**, *46*, 5897.
(48) Davis, K. P.; Lodge, T. P.; Bates, F. S. *Macromolecules* **2008**, *41*, 8289.
(49) Pispas, S.; Sarantopoulou, E. *Langmuir* **2007**, *23*, 7484.
(50) Yu, Y.; Eisenberg, A. *J. Am. Chem. Soc.* **1997**, *119*, 8383.
(51) Yu, Y.; Zhang, L.; Eisenberg, A. *Langmuir* **1997**, *13*, 2578.
(52) Yu, K.; Eisenberg, A. *Macromolecules* **1996**, *29*, 6359.
(53) Tung, P. H.; Kuo, S. W.; Jeong, K. U.; Cheng, S. Z. D.; Huang, C. F.; Chang, F. C. *Macromol. Rapid Commun.* **2007**, *28*, 271.

JP901398E